

# Mineral Particles Internally Mixed with Sea Salt over Karatsu Bay, Southwest of Japan, Observed with a Small Unmanned Aerial Vehicle

Masahiko HAYASHI<sup>1)</sup>, Yoshiteru KAMIYA<sup>1)</sup>, Keiichi OZUKA<sup>1,3)</sup>, Katsuya YAMASHITA<sup>1,4)</sup>,  
Hitomi HIGASHI<sup>1)</sup>, Masami ASHIDA<sup>1)</sup>, Kazuo OKABE<sup>2)</sup>, and Tetsuo SHIGETA<sup>2)</sup>

(Received May 31, 2010)

## Abstract

Observations of aerosols in the boundary layer over Karatsu Bay were performed at northern Kyushu, Japan, in the spring seasons of 2004 and 2005. Vertical profiles of aerosol number concentrations were observed with an optical particle counter, and aerosol particles were collected with an airborne impactor, on board a small unmanned aerial vehicle, called Kite Plane. Single particle analyses performed using a scanning electron microscope and X-ray spectrometer show that the particle of internal mixture of mineral and sea salt is one of the dominant types of aerosol larger than 1  $\mu\text{m}$  in diameter. These particles were sometimes found in air masses that had not experienced cloud activities. Ratios of the internal mixture particles of sea salt and mineral to total mineral particles were higher in mixed layers with temperature higher than that of the sea surface, suggesting that sea fog played a key role in their production.

Key words: Internal Mixture, Mineral Particle, Sea Salt, Mixed Layer, Sea Fog, Sea Surface Temperature, Unmanned Aerial Vehicle, Kite Plane

## 1. Introduction

The Asian continent is one of the world's largest sources of aeolian dust and other land-originated aerosols. Aeolian dust from arid regions of the Asian continent spreads over the Pacific Ocean and sometimes reaches North America<sup>1), 2)</sup>. It affects global material circulation, biogenic cycles, and radiation budgets. It also interacts with various atmospheric trace gases and water vapor. Some investigators have shown that particles internally

mixed with mineral and sea salt, hereafter called MS particles, frequently exist, and are found over the remote Pacific Ocean<sup>3)</sup>. This transformation causes changes in the dynamical, chemical, and radiative features of mineral particles. A high fraction of MS particles in Kyushu Island, near China was observed and suggested that cloud processes played a role in their production<sup>4), 5), 6)</sup>. Zhang et al. also showed that fraction of Asian dust with sea salt at ground level increased with deep convection of lower atmosphere in southwest of Japan. On the other hand, it was

<sup>1)</sup> Faculty of Science, Fukuoka University, 8-19-1 Nanakuma, Jonan-ku, Fukuoka, 814-0180, Japan

<sup>2)</sup> Sky Remote Co. Ltd, Kumamoto, Japan

<sup>3)</sup> Nippon Tungsten Co. Ltd, Fukuoka, Japan

<sup>4)</sup> Now, Meteorological Research Institute, Tsukuba, Japan

shown that the mixture was frequently found in air masses which had not experienced cloud activities<sup>7, 8)</sup>. Yamashita et al.<sup>8)</sup> pointed out the possibility of sea fog as the formation process of MS particles in the boundary layer, based on observations in the upper boundary layer using a small unmanned aerial vehicle called Kite Plane. These studies suggested that MS particles were formed between China and Japan. However, there are few observations, especially of the vertical distribution of MS particles in the entire boundary layer, and the mechanism of MS particle formation has been unclear.

This study presents the vertical variation of MS particles observed in spring at northern Kyushu using a Kite Plane, and discusses the processes of producing MS particles.

## 2. Observation and instrumentation

### 2.1 The platform: Kite Plane

A Kite Plane (KP: Sky Remote Co. Ltd) was used as the observation platform. KPs have been increasingly used for observations of atmospheric aerosols<sup>8, 10, 11)</sup> and trace gases<sup>12)</sup>. The advantages of KPs for aerosol measurements are: 1) they are easy to be controlled, 2) they have a relatively large payload (up to 5 kg), 3) they have a slow cruise speed (about 10 m/s with 100 m/min speed of ascent), 4) they are robust and resistant to accidental damage, and 5) there is no contamination by motor exhaust. KPs are able to be operated by automatic controllers for trace gas measurements<sup>12)</sup>. However, the KPs with old automatic controllers restricted payload to less than 3 kg and cruise duration to one hour. A new automatic control system, simple and lightweight (1.7 kg), was developed for this program<sup>10, 11)</sup>. It is constructed from an H8 CPU board, Global Positioning System, and Spread Spectrum telecommunication system. The new KP can cruise up to 3.0 km in altitude for two hours, with a 6.0 kg payload.

### 2.2 Instrumentation

An optical particle counter (OPC: YGK Co. Ltd.) and an aerosol sampler (Arios Co. Ltd.) were mounted on the KP. Measurements of pressure, temperature and relative humidity were made using a piezo sensor, residence thermistor, and hipolymer

thin film sensor, respectively. The horizontal position of the KP was monitored with the GPS, and the altitude was calculated using the hydrostatic approximation with measured temperatures and pressures.

The OPC has two independent optical systems, both measuring aerosol number concentrations and size distributions. The two systems have cross angles (between light source axis and collecting optics axis) of 60° and 90°, respectively. Each system has size counters with discriminator corresponding to spheres of diameter 0.3, 0.5, 1.0, 2.0, 5.0  $\mu\text{m}$  for refractive index of 1.59-0i. Sample air is introduced with flow rate of 300  $\text{cm}^3/\text{min}$ . The OPC accumulates the number of electric pulses converted from scattered light, corresponding to the number of particles, every 4 s. Statistical error of one standard deviation is about 10% for 5 particles/ $\text{cm}^3$  in raw data. In this paper we show only the results obtained by the optics of 60°.

A two-stage cascade impactor, originally developed for balloon-borne observations in the stratosphere<sup>14)</sup>, is used as the sampler for elemental composition analyses of individual particles. Sampling flow rate is 1.5 l/min, and jet diameters of the first and the second stage are 1.3 mm and 0.5 mm, respectively. Assuming a density of aerosol particles of 2.0  $\text{g}/\text{cm}^3$ , 50% cutoff diameters for the first and the second stage are 1.0  $\mu\text{m}$  and 0.2  $\mu\text{m}$ , respectively. The sampler can collect 16 pairs of samples in one flight.

Inlet tubes were placed at the nose of the KP such that they would be directed parallel to streamlines of ambient air flow. Thus, air is introduced directly to the OPC and sampler from the front of the KP. Number concentration and size distribution are not modified artificially during the sampling procedure.

### 2.3 Observations

Two sites were used for observations (Fig. 1). One is Nijino-Matsubara (33°27'N, 130°00'E, on the shore of Karatsu Bay) for vertical structure observations, using the KP. Instruments for the ground based station were installed nearby, and the grassed seashore was used as a runway. The second site was a sightseeing observatory (33°26'N, 130°01'E, 280 m above sea level) on Mt. Kagamiyama. This site is located at the top of a steep slope, 2 km

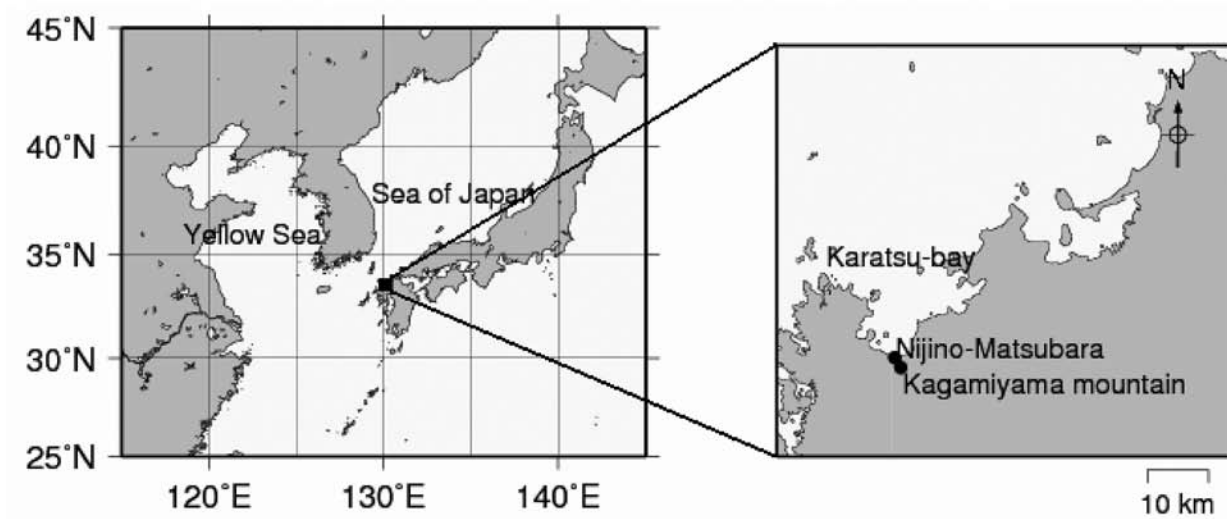


Figure 1 Observation site for Kite Plane operation, Nijino-Matsubara, and the mountain base observation site, Mt. Kagamiyama.

Table 1 Record of Flights and Observations

year	m/dd	platform	OPC observation		Sampling	
			time	Max altitude (m)	time	altitude (m)
2004	3/25	Kite Plane	10 : 20 - 11 : 17	1630	10 : 31~10 : 34	300
	3/27	Kite Plane	8 : 31 - 10 : 07	2420	9 : 53~ 9 : 56	300
	4/1	Mountain		280	11 : 05~11 : 06	280
	4/24	Kite Plane	10 : 18 - 11 : 27	1510	10 : 58~11 : 03	1450
					11 : 08~11 : 13	800
		Kite Plane	11 : 56 - 13 : 19	2120	12 : 43~12 : 45	2100
				12 : 55~13 : 00	1400	
	4/25	Kite Plane	10 : 45 - 12 : 27	2010	11 : 47~11 : 52	300
2005	3/25	Mountain		280	11 : 11~11 : 14	280
	3/30	Kite Plane	9 : 31 - 11 : 18	1620	10 : 45~10 : 50	800
					11 : 01~11 : 06	300
	3/31	Kite Plane	9 : 27 - 11 : 02	1330	9 : 51~ 9 : 55	800
					10 : 03~10 : 07	300
	4/2	Kite Plane	9 : 30 - 10 : 27	1160	10 : 16~10 : 20	300
4/4	Kite Plane	10 : 09 - 11 : 48	1560	10 : 56~11 : 00	1000	
				11 : 11~11 : 15	300	

southeast from Nijino-Matsubara. This site was used to collect data and samples at 280 m above sea level by ground base operations if the KP could not be operated.

The KP took off from a seashore area 25 m wide and cruised over Karatsu Bay. The flight range was less than 2 km. Observations were performed during

the morning. Altitudes for collection of aerosol particles were determined by the vertical profiles of temperature, humidity, and size distribution of aerosols during ascent. While the KP was descending, the KP held constant altitude for several minutes at each sampling level, and aerosol particles were collected by command from the ground. The

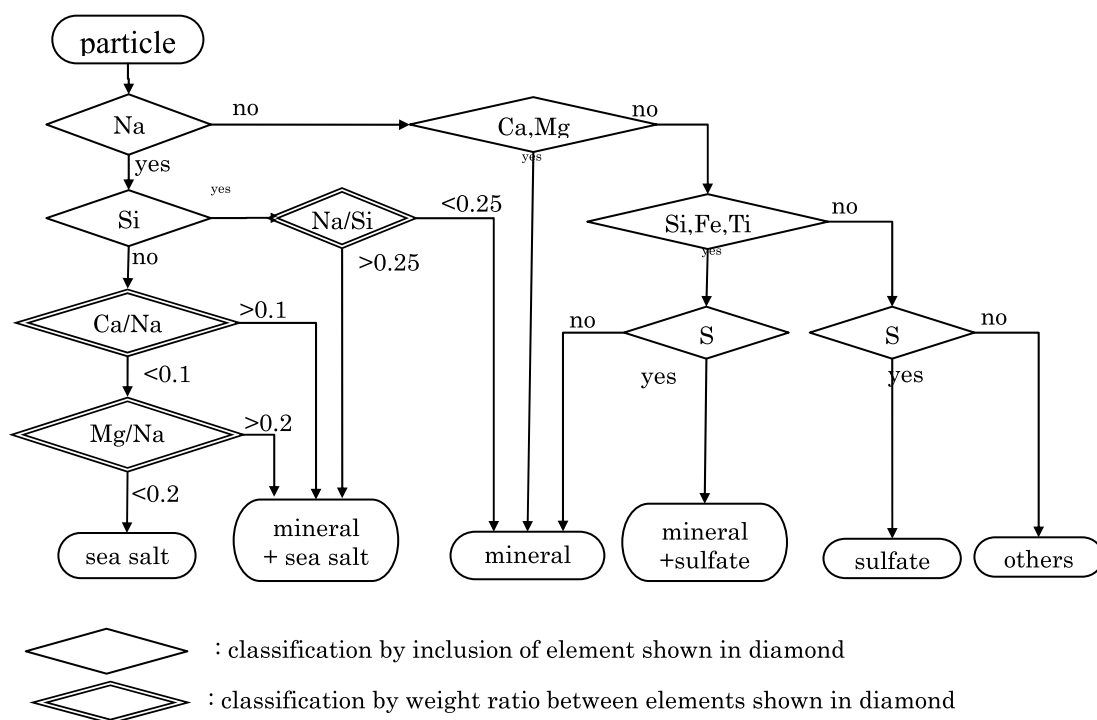


Figure 2 Particle classification diagram.

automatic control system held constant altitude within a tolerance of  $\pm 30$  m.

Sixteen flights and five mountain-based observations were carried out successfully, and 37 pairs of samples were collected. Here we show the results of analyses of 16 samples of them, shown in Table 1.

### 3. Analyses

The morphology and elemental compositions of individual particles were analyzed with a Scanning Electron Microscope (SEM: Quanta FEG200, FEI Co. Ltd.) equipped with an energy-dispersed X-ray spectrometer (EDX: Genesis 4000, EDAX Co. Ltd.). Particles whose diameters were larger than  $1.0 \mu\text{m}$ , collected in the first stage, were analyzed. More than 50 particles were randomly selected and analyzed for each sample plate. The X-ray spectra were generated from exposed areas of the particles for 50 seconds with an accelerator voltage of 20 kV. The weight fractions of elements in individual particles were calculated using the ZAF (Z: element atom number; A: absorption; F: fluorescence) correction. C, N, and O were excluded from quantitative analyses

because of the poor accuracy of light elements.

Individual aerosol particles analyzed by SEM-EDX were classified into six types (M: mineral; MS: mineral + sea salt; MF: mineral + sulfate; S: sea salt; F: sulfate; and O: others) using the chart in Fig. 2. Particles containing Ca and/or Mg without Na were classified as mineral. Particles containing only Si, Al, Ti, and Fe were also considered to be mineral, and those with S were mineral + sulfate. Using the criterion presented by Niimura<sup>4)</sup>, particles containing Na and Si with Na/Si weight ratio above 0.25, were classified into mineral + sea salt particles, even if Cl was not detected and those with weight ratio below 0.25 were considered to be mineral particles. Particles containing Na but not Si with Ca/Na weight ratio below 0.1 and Mg/Na weight ratio below 0.2 were classified as sea salt particles (including transformed sea salt particles), and those with weight ratio above 0.1 for Ca/Na or 0.2 for Mg/Na were classed as mineral + sea salt.

Backward trajectories, cloud images and humidity profiles of routine radiosondes were used to determine the history of cloud activities along the path of the observed air parcels over Karatsu Bay, following the method of Yamashita et al.<sup>8)</sup>. Backward

Table 2 Summary of aerosol concentration and classification

Sample ID yymmdd-alt.	particle concentration (/liter)		Fraction (%) of aerosol type for $d > 1.0 \mu\text{m}$						number of analyzed particles
	0.3<d<1.0	d>1.0	Mineral	Mineral + Sea	Mineral + Sulfate	Sea salt	Sulfate	Others	
			M <sup>#</sup>	MS <sup>#</sup>	MF <sup>#</sup>	S <sup>#</sup>	F <sup>#</sup>	O <sup>#</sup>	
040325- 300	202393	1946	62	15	0	16	2	5	106
040327- 300	41215	410	36	9	3	10	5	38	104
040401- 280	79878	3494	25	1	0	29	1	35	106
040424-1450	70031	8029	50	24	0	24	0	2	50
040424- 800	50443	8978	26	48	0	26	0	0	50
040424-2100	27437	1466	76	10	0	12	2	0	50
040424-1400	98840	8670	60	20	0	20	0	0	50
040425- 300	80320	1460	64	8	1	21	1	5	107
050325- 280	43862	2269	75	2	0	5	3	15	105
050330- 800	102167	4941	38	14	0	44	0	4	50
050330- 300	97392	4758	14	31	1	51	0	3	109
050331- 800	304728	6924	29	20	1	43	4	3	106
080331- 300	222330	5835	30	19	0	46	0	6	107
050402- 300	91038	2238	35	25	2	29	1	8	106
050404-1000	68585	935	11	8	0	79	0	2	102
050404- 300	66066	1296	6	11	0	79	1	3	107

# : ID for aerosol type representation

trajectories were calculated using HYSPLIT (NOAA, <http://www.arl.noaa.gov/ready/hysplit4.html>). Relative humidity profiles, at routine meteorological sonde stations obtained from the University of Wyoming website (<http://weather.uwyo.edu/upperair/sounding.html>), were used to determine the vertical distribution of cloud activity. Visible and infrared cloud images (Kouchi University, <http://weather.is.kouchi-u.ac.jp/>), observed by GOES-9 and analyzed by the Meteorological Satellite Center of JMA, were used to obtain the horizontal distribution of cloud along the pathway of the air mass in which mineral particles were sampled.

## 4. Results and discussion

### 4.1 Fraction of internal mixture of mineral and sea salt

Table 2 shows the number concentration observed with OPC and the fraction of each aerosol type analyzed with SEM-EDX. The column of Sample ID shows sampling dates and altitudes in meters.

The next column shows the number concentrations of the accumulation mode, 0.3–1.0  $\mu\text{m}$  in diameter, and primary mode, larger than 1.0  $\mu\text{m}$  in diameter. The fraction of aerosol particles, hereafter shown as F (ID of aerosol type), was derived from SEM-EDX analyses. It shows that dominant particles in the primary mode are mineral (M), sea salt (S), and internal mixture of mineral and sea salt (MS).

The lower troposphere is usually divided into free troposphere and boundary layer, and the boundary layer is divided further into mixed layer, residual layer, and transition layer. The mixed layer is affected locally and strongly by surface conditions and emissions. Here, the sublayers to which air parcels belong are identified by the vertical profile of potential temperature, water mixing ratio, and particle concentrations<sup>8</sup>). These profiles were obtained from in-situ observations of KP flight and routine meteorological balloon observations by Japanese Meteorological Agency at Fukuoka, 50 km east from sampling area. The layer with large gradient of potential temperature (larger than

Table 3 Summary of layer classification and air mass history

Sample ID yymmdd-alt.	layer class	cloud image overlap	Relative humidity observed by sonde		possibility of cloud experiment	days over sea
			station <sup>(2)</sup>	max.humidity		
040325- 300	residual	no	PF, BN	30	low	4.5
040327- 300	residual	yes	YJ, CC	65	low	1.4
040401- 280	residual	no	OS, BJ	20	low	1.5
040424-1450	residual	no	OS, SY	65	low	0.8
040424- 800	mixed	no	OS, SY	65	low	1.2
040424-2100	free trop.	no	OS	65	low	0.5
040424-1400	residual	no	OS, SY	60	low	1.2
040425- 300	mixed	no	PH, OS, SY	50	low	1.5
050325- 280	mixed	yes	KG, YZ	70	in fog <sup>(1)</sup>	0.8
050330- 800	residual	no	OS, SY	35	low	1.0
050330- 300	mixed	no	OS, DD, CC	50	low	1.0
050331- 800	residual	yes	KG, QD, BJ	85	high	1.3
050331- 300	mixed	no	KG, QD, BJ	25	low	2.0
050402- 300	residual	yes	KS, KG, QD, BJ	60	low	3.0
050404-1000	residual	no	YJ, YC	30	low	1.0
050404- 300	mixed	yes	PH, SC, YJ	90	high	1.5

(1) sampling was carried out in fog

(2) Station ID; YC (Yichun, 47°43'N, 128°54'E), CC (Changchun, 43°54'N, 125°13'E), YJ (Yanji, 42°53'N, 129°28'E), SY (Shengyang, 41°46'N, 123°26'E), JZ (Jinzhou, 41°07'N, 121°04'E), DD (Dandong, 40°05'N, 124°20'E), BJ (Beijing, 39°56'N, 116°17'E), SC (Sokcho, 38°15'N, 128°34'E), BN (Baengnyeongdo, 37°58'N, 124°38'E), OS (Osan, 37°06'N, 127°02'E), QD (Qingdao, 36°04'N, 120°20'E), PH (Pohang, 36°02'N, 129°23'E), KG (Kwangju, 35°07'N, 126°49'E), KS (Kagoshima, 31°33'N, 130°33'E)

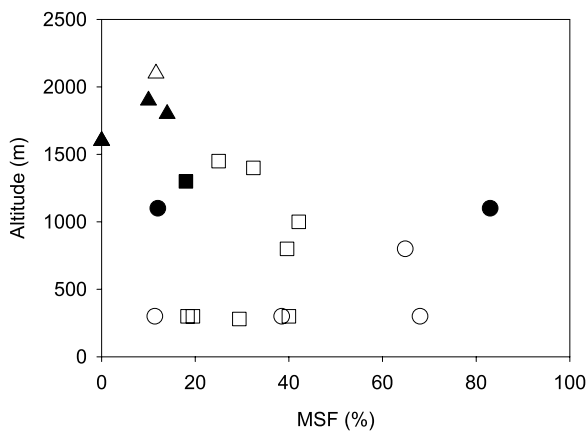


Figure 3 Vertical distribution of fraction of internal mixture of mineral and sea salt (MSF).

- circle: mixed layer
- square: residual layer
- triangle: free troposphere
- open symbol: this study
- solid symbol: data from Yamashita et al.<sup>(8)</sup>

1 K/km), and low relative humidity (less than 20%) is classified as free troposphere. Boundary sublayer with constant potential temperature, mixing ratio and particle mixing ratio from the ground is classified as mixed layer, and the layer between free troposphere and boundary layer is considered as the residual layer. The layer classes of air mass for sampling and analyses are shown in Table 3.

The history of cloud formation activities within the air masses was determined as described in Section 3, and the results are given in Table 3. These show that most of samples have not experienced cloud activity.

Here we define the fraction of MS particles to all of mineral particles as MSF:

$$MSF = F(MS) / (F(M) + F(MS) + F(MF)) \quad (1)$$

where F(X) means fraction of type X of particle as shown in Table 2.

Figure 3 shows the vertical distribution of

MSF calculated from **Table 2** and equation (1), but doesn't include samples that have a high probability of experiencing cloud. Layer classes are shown by symbols in Fig. 3. Values of MSFs shown by solid symbols in **Fig. 3** are those over Mt. Raizan reported by Yamashita et al.<sup>8)</sup>. The mountain is located 20 km east of Nijino-Matsubara, and its elevation is 780 m above sea level. The vertical distribution shows that MSF is variable, from zero percent up to 82 %, in the spring over the Japan Sea coast. **Figure 3** also reveals that MS particles are not dominant above 1500 m, which are defined as free troposphere, as described above.

**Table 3** and **Figure 3** show that the air mass around 300 m in altitude sometimes belongs to the mixed layer and sometimes to the residual layer. It is clear that the variation of MSF in the boundary layer, mixed layer and/or residual layer, is very large and does not depend on altitude or layer class.

#### 4.2 Conditions to form internal mixture in mixed layer

**Table 2** and **Table 3** show that correlation between MSF in boundary layer and traveling period over the sea is very weak and there are any other processes to control MSF. Niimura et al.<sup>6)</sup> and Yamashita et al.<sup>8)</sup> show that Brownian motion and turbulence can not explain the effective formation shown in **Table 3** and **Fig. 3**. In addition, Yamashita et al.<sup>8)</sup> proposed that coagulation by Coulomb forces between electrically charged particles may act as another possible formation process. Production rates of such a process are roughly represented by the following relation:

$$dN(XY)/dt = K \times N(X) \times N(Y) \quad (2)$$

where K is the collision factor and N is the number concentration of particles of category X, Y and XY (internal mixture of X and Y).

The initial condition of  $N_0$  for N(M) and N(S) is unknown. We assume that all particles are not scavenged and obtain a relation as follows:

$$\begin{aligned} N_0(S) &= N(S) + N(MS) \\ N_0(M) &= N(M) + N(MS) + N(MF) \end{aligned} \quad (3).$$

We assume N(X), as the product of total number concentration ( $N_p$ ) and F(X), shown in **Table 3**.

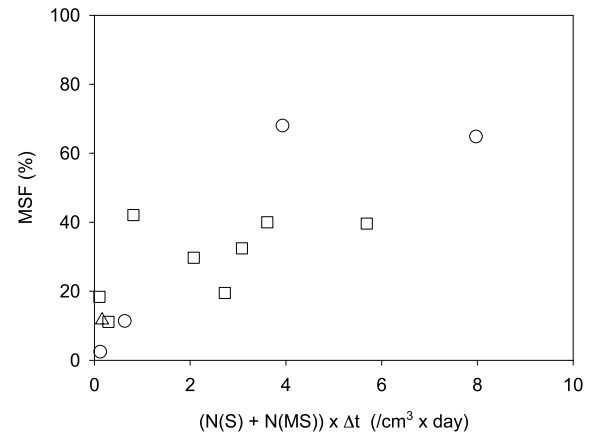


Figure 4 Correlation between MSF and sea salt concentration times  $\Delta t$  (travel time over sea). Symbols are the same as in Figure 3.

Then we obtain number concentration of MS particles,  $N(MS)$ , at  $\Delta t$  after the initial condition:

$$N(MS) = K \times N_0(M) \times N_0(S) \times \Delta t + N_0(MS) \quad (4).$$

Then we obtain the following relation, assuming no internal mixture of mineral and sea salts at initial condition,  $N_0(MS) = 0$ :

$$\begin{aligned} MSF &= \frac{N(MS)}{N(M) + N(MS) + N(MF)} \\ &= K \times (N(S) + N(MS)) \times \Delta t \end{aligned} \quad (5).$$

This suggests that MSF is proportional to  $(N(S) + N(MS)) \times \Delta t$ , if collision coefficient is constant. **Figure 4** shows the correlation between observed MSF and  $(N(S) + N(MS)) \times \Delta t$ . The correlation is very weak, and it is difficult to explain MS particle production by coagulation between mineral particle and sea salt particle by Coulomb forces.

Yamashita et al.<sup>8)</sup> also pointed out the possibility of the formation of internal mixture of mineral and sea salt through sea fog activity. Turbulent sea fog is formed when a cold air layer contacts a warm sea surface<sup>14)</sup>. Sea fog is frequently observed over northwestern North Pacific and acts as scavenging process of chemical constituents and aerosols<sup>15)</sup>. **Figure 5** shows the relation between MSF and potential temperature at sampling altitude. The

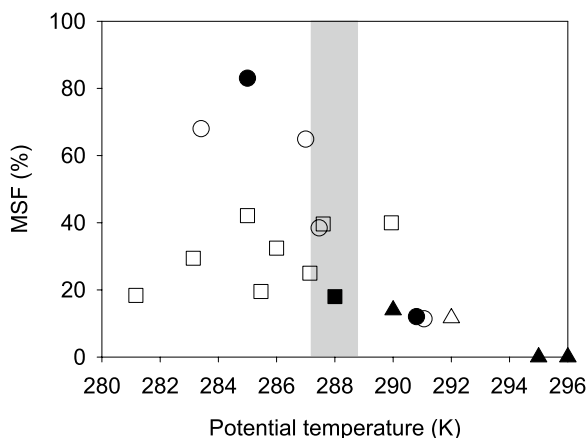


Figure 5 Correlation between MSF and potential temperature. Gray area shows sea surface temperature between Kyushu and the Korean Peninsula. Symbols are the same as in Figure 3.

range of daily mean sea surface temperatures (SST) between Kyushu and the Korean Peninsula during observation is shown by gray hatching. These are obtained from daily mean SST data observed by the Japan Meteorological Agency ([http://www.data.kishou.go.jp/kaiyou/db/kaikyo/daily/sst\\_wnp.html](http://www.data.kishou.go.jp/kaiyou/db/kaikyo/daily/sst_wnp.html)). Sea surface temperature around the area is the highest along the track of air mass to the observation area. Figure 5 shows that MSF is higher in the cold mixed layer overlying warmer seawater but MSFs in the residual layer do not depend on difference between temperature of sampling level and SST. It is difficult to identify sea fog and low-level cloud from satellite images, and also difficult to discriminate between them, as the two are similar physical phenomena. However, these results suggest that the presence of sea fog and/or low-level cloud contributes to the formation of internal mixture of mineral and sea salt.

## 5. Summary

Analysis of the elemental composition of aerosols in the boundary layer over coastal northern Kyushu conducted in the spring seasons of 2004 and 2005 with a Kite Plane, small UAV, found the following results.

1. Internal mixture particles of mineral and sea salt (MS) were found in the boundary layer, and the ratio to mineral particles ranged from

20 to 90%.

2. Number fractions of MS particles in the residual layer were around 10-40%, while those in free troposphere were less than 10%.
3. Number fractions of MS particle in the mixed layer were variable, but generally between 60 to 90%.
4. Number fractions of MS particles showed no correlation with number concentrations of sea salt particles, but they were enhanced in the cold air layer overlying a warmer sea surface in the study area, off the west coast of Japan.

These suggest that sea fog and/or low-level cloud play an active role in the formation of MS particles.

## Acknowledgments

This study was undertaken as part of the ADEC Project (Aeolian Dust Experiment on Climate Impact) sponsored by the Ministry of Education, Culture, Sports, Science and Technology of the Government of Japan. This study was also supported by the Ministry of Education, Culture, Sports, Science and Technology of the Government of Japan under a Grant-in-Aid for Scientific Research on a Priority Area (Grant 14048225).

## References

- 1) Duce, R.A., Unni, C.K., Ray, B.J., Prospero, J.M., and Merrill, J.T.: Long-range atmospheric transport of soil dust from Asia to the tropical North Pacific, *Science*, **209**, 1522-1524 (1980).
- 2) Shaw, G.E.: Transport of Asian Desert Aerosol to Hawaiian Island, *J. Appl. Meteor.*, **19**, 1254-1259 (1980).
- 3) Andreae, M.O., Charlson, R.J., Bruynseels, F., Strom, H., Grieken, R.V., and Maenhaut, W.: Internal mixture of sea salt, silicates, and excess sulfate in marine aerosols, *Science*, **232**, 1620-1623 (1986).
- 4) Niimura, N., Okada, K., Fan, X.-B., Kai, K., Arai, K., and Shi, G.-Y.: A method for the identification of Asian dust-storm particles mixed internally with sea salt, *J. Meteorol. Soc. Japan*, **72**, 777-784 (1994).
- 5) Fan, X.-B., Okada, K., Niimura, N., Kai, K., Arai,

- K., Shi, G.-Y., and Mitsuta, Y.: Mineral particles collected in China and Japan during the same Asian dust-storm event, *Atmos. Environ.*, **30**, 347-351 (1996).
- 6) Niimura, N., Okada, K., Fan, X.-B., Kai, K., Arai, K., Shi, G.-Y., and Takahashi, S.: Formation of Asian dust-storm particles mixed internally with sea salt in the atmosphere, *J. Meteorol. Soc. Japan*, **76**, 275-288 (1998).
  - 7) Zhang, D., Iwasaka, Y., Shi, G., Zang, J., Matsuki, A., and Trochkin, D.: Mixture state and size of Asian dust particles collected at southwestern Japan in spring 2000, *J. Geophys. Res.*, **108(D24)**, 4760, doi:10.1029/2003JD003869 (2003).
  - 8) Yamashita, K., Hayashi, M., Irie, M., Yamamoto, K., Saga, K., Ashida, M., Shiraishi, K., and Okabe, K.: Amount and state of mineral particles in the upper mixed layer and the lower free troposphere over Mt. Raizan, southwestern Japan: Unmanned airplane measurements in the spring of 2003, *J. Meteorol. Soc. Japan*, **83**, 121-136 (2005).
  - 9) Zhang, D., Iwasaka, Y., Matsuki, A., Ueno, K., and Matsuzaki, T.: Coarse and accumulation mode particles associated with Asian dust in southwestern Japan, *Atmos. Environ.* **40**, 1205-1215 (2006).
  - 10) Hayashi, M., Yamashita, K., Morimoto, K., Yamamoto, T., Shi, G., and Chen, B.: Plan for Aeolian dust measurements in the upper atmosphere with unmanned airplane, *Proc. First ADEC Workshop, Yokohama*, S3-2 (2002).
  - 11) Hayashi, M., Yamashita, K., Ozuka, K., Shiraishi, K., Otobe, N., Yamamoto, T., Chen, B., and Shi, G.-Y.: Variation of size distribution and mineral composition of Aeolian dust in the boundary layer at DunHuang, China: Unmanned airplane measurement in spring and summer from 2002 to 2004, *Proc. Fourth ADEC Workshop, Nagasaki*, 247-249 (2005).
  - 12) Watai, T., Machida, T., Ishizaki, N., and Inoue, G.: A lightweight observation system for atmospheric carbon dioxide concentration using a small unmanned aerial vehicle, *J. Atmos. Oceanic Technol.*, **23**, 700-710 (2006).
  - 13) Okada, K., Wu, P.-M., Tanaka, T., and Hotta, M.: A light balloon-borne sampler collecting stratospheric aerosol particles for electron microscopy, *J. Meteorol. Soc. Japan*, **75**, 753-760 (1997).
  - 14) Fukuchi, A.: "Lecture on the marine weather", 8th ed., Seizandou Syoten, 355 (2003) (in Japanese).
  - 15) Sasakawa, M., Ooki, A., and Uematsu, M.: Aerosol size distribution during sea fog and its scavenge process of chemical substances over the northwestern North Pacific, *J. Geophys. Res.*, **108(D3)**, doi:10.1029/2002JD002329 (2003).

